Supporting Information

^{90}Sr bioassay in small-volume urine by ICP-MS/MS with CO_2 as the reaction gas

Guosheng Yang[a,*], Hirofumi Tazoe[b], Eunjoo Kim[a], Jian Zheng[a], Munehiko Kowatari[a], Osamu Kurihara[a]

[a] National Institutes for Quantum Science and Technology (QST), 4-9-1 Anagawa, Inage, Chiba 263-8555, Japan

[b] Institute of Radiation Emergency Medicine, Hirosaki University, 036-8564, Aomori, Japan

*Corresponding author. E-mail address: yang.guosheng@qst.go.jp

PROCORAD inter-comparison

Each year around 30 laboratories, including ours at QST, Japan, participate in the inter-comparison exercises for ^{90}Sr in urine offered by PROCORAD (Association for the PROmotion of Quality COntrol in RADiotoxicological Analysis).

For the PROCORAD intercomparison campaign 2020, three urine samples spiked with or without ^{90}Sr (20 SRA, 20 SRB, and 20 SRC) were sent to our laboratory. For the PROCORAD intercomparison campaign 2023, three urine samples spiked with or without ^{90}Sr (23 SRA, 23 SRB, and 23 SRC) were sent to our laboratory. For each sample, a total of approximately 70 L of urine was collected from each healthy human volunteer who was not subject to any risk of radioactive contamination.

After confirming that there was no detectable ^{90}Sr in the collected urine, the urine (ca. 500 mL) was fractionated in flasks and each flask was spiked individually with certified source prior to sending the samples to participating PROCORAD laboratories.

Chemical and chromatographic purification for beta counting analysis

As shown in Fig. S1, 500 mL urine was transferred into glass beaker and 50 mL concentrated HNO_3 was added. Sample bottle was rinsed three times with 5 mL concentrated HNO_3. After heating the mixture to dryness at 140 ^{o}C, 5 mL concentrated HNO_3 and 2 mL of 30% H_2O_2 were added, and this mixture was heated to dryness at 140 ^{o}C to decompose organic matter. This step was repeated 4 times to obtain totally white residue. Subsequently, the final residue was re-dissolved into 20 mL concentrated HNO_3 by heating at 120 ^{o}C for 30 min with watch glass. After that, the solution was filtrated with 0.45 μm pore PTFE membrane filter. The glass beaker was rinsed with ultrapure water and the solution was also filtrated. Finally, solution volume of 100 mL was obtained for next purification. The solution was left for waiting for > two weeks to obtain the secular equilibrium of ^{90}Sr - ^{90}Y. After that, 4 mL solution was taken out from the 100 mL HNO_3 solution mentioned above, and 1 mL of 1 mg/mL stable Y standard solution was added as carrier. Then, 2 mL concentrated HNO_3 was added for loading on 1 mL DGA resin cartridge. The resin cartridge was rinsed with 10 mL 8 M HNO_3 with a flow rate of 2 mL min^{-1}, then with 10 mL 8 M HCl to remove Bi, 20 mL

3 M HNO_3 and 0.3 M HF to remove U and Th, 20 mL 0.02 M HNO_3 to remove La, Ce and other light rare earth elements. Finally, Y was eluted with 20 mL 0.1 M HCl. A 100 μL of the Y fraction was taken out and diluted to 10 mL with 2% HNO_3 for analysis by inductively coupled plasma-optical emission spectrometry (SPECTRO BLUE, SCP SCIENCE, Quebec, Canada) to obtain the recovery. For the residual solution, 1 mg Fe carrier purified from $FeCl_3 \cdot H_2O$ (reagent-grade, Wako Chemical, Japan) was added and the precipitation was performed with addition of 0.3 mL aqueous NH_4OH. After filtrating the precipitation on a mixed cellulose esters membrane and drying the precipitation with infrared lamp, the precipitation was placed onto an acrylic holder and wrapped with PE film. Finally, the activity of ^{90}Y was analyzed with the beta counting of the low background 2 π gas flow proportional counter for 60 h.

Table S1 The daily ^{90}Sr content in urine associated with the specified committed effective dose (1 mSv) and the required limits of detection based on the assumption of a daily excretion of 1.6 L for an adult male, using 10 mL urine for analysis, and the final analytical solution volume of 1 mL for ICP-MS analysis.

	[a]Urinary excretion (Bq/d)			Concentration (Bq/L)			Detection required (Bq/mL)		
Inhalation type	Day 1	Day 2	Day 3	Day 1	Day 2	Day 3	Day 1	Day 2	Day 3
Fast	1800	870	540	1125	544	338	11.3	5.44	3.38
Moderate	400	240	150	250	150	93.8	2.50	1.50	0.938
Slow	1.9	1.1	0.69	1.19	0.69	0.43	0.012	0.007	0.004
Ingestion	1600	670	430	1000	419	269	10.0	4.19	2.69
	Urinary excretion (pg/d)			**Concentration (pg/L)**			**Detection required (ng/L)**		
	Day 1	Day 2	Day 3	Day 1	Day 2	Day 3	Day 1	Day 2	Day 3
Fast	352	170	106	220	106	66	2.20	1.06	0.66
Moderate	78.2	46.9	29.3	48.9	29.3	18.3	0.489	0.293	0.183
Slow	0.372	0.215	0.135	0.232	0.134	0.084	0.00232	0.00134	0.00084
Ingestion	313	131	84.1	196	81.9	52.6	1.96	0.819	0.526

[a] The ^{90}Sr excretion content in urine is calculated from OIR Data Viewer software.

Table S2 Potential polyatomic/isobaric interferences and major matrix elements for ^{90}Sr analysis in urine by ICP-MS/MS.

Interfering element	Interference	Abundance of former isotope	Abundance of latter isotope	Required resolution	Median	Geometric mean	95th percentile		Amount in 10 mL urine
		%	%		ng/mL	ng/mL	ng/mL	ng/mL	ng
Ti	$^{50}Ti^{40}Ar^{+}$	5.18	99.6	1.60×10^{5}	5.14		12.19		122
V	$^{50}V^{40}Ar^{+}$	0.25	99.6	4.98×10^{4}	1.58		3.79		37.9
Cr	$^{50}Cr^{40}Ar^{+}$	4.345	99.6	1.30×10^{5}	0.35		0.79		7.9
	$^{52}Cr^{38}Ar^{+}$	83.79	0.06	2.00×10^{4}					
	$^{54}Cr^{36}Ar^{+}$	2.365	0.34	6.85×10^{4}					
Mn	$^{55}Mn^{35}Cl^{+}$	100	75.76	1.07×10^{5}			0.46		4.6
Fe	$^{54}Fe^{36}Ar^{+}$	5.85	0.34	1.54×10^{5}				24	240
Ni	$^{58}Ni^{16}O_2^{+}$	68.08	99.76	5.16×10^{3}	1.99		6.35		63.5
Ge	$^{72}Ge^{18}O^{+}$	27.31	0.2	6.66×10^{3}	0.65		2.62		26.2
	$^{74}Ge^{16}O^{+}$	36.72	99.76	1.08×10^{4}					
	$^{76}Ge^{14}N^{+}$	7.83	99.64	5.37×10^{3}					
Se	$^{74}Se^{16}O^{+}$	0.89	99.76	9.31×10^{3}	13.4		33.39		334
	$^{76}Se^{14}N^{+}$	9.37	99.64	6.18×10^{3}					
	$^{78}Se^{12}C^{+}$	23.77	98.93	9.39×10^{3}					
Y	$^{89}Y^{1}H^{+}$	100	99.99	1.51×10^{4}	<0.059				
Zr	$^{90}Zr^{+}$	51.45		2.96×10^{4}	<0.945				
Sr						144	506		5060
Major element					**µg/mL**	**µg/mL**	**µg/mL**		**mg**
Na					2104	1928	5078		50.8
Mg					71	57	191		1.91

K	2569	2244	6780	67.8
Ca	76	76	309	3.09

All the data are cited from Morton et al., 2014,[1] except for the data of Fe from Nakagawa et al., 2004 [2] and Sr from Usuda et al., 2006.[3]

Table S3 Instrumental and data acquisition settings for ICP-MS/MS (Agilent 8900 ICP-QQQ)

Instrumental settings	
Sample cone	S type
Skimmer cone	S type
Nebulizer	Conical concentric
RF power	1550 W
RF matching	1.20 V
Sampling position	8.0 mm
Carrier gas	0.90 L/min
Makeup gas	0.14 L/min
Nebulizer pump	0.1 rps
Extraction lens 1	4.2 V
Extraction lens 2	-240.0 V
Omega bias	-110 V
Omega lens	10.0 V
Q1 entrance	0 V
Q1 exit	2.0 V
Cell focus	3.0 V
Cell entrance	-70 V
Cell exit	-120 V
Deflection	5.0 V
Plate bias	-80 V
Data acquisition settings	
Q2 peak pattern	6 points
Replicates	5
Sweep/Replicates	300
Scan mode	MS/MS
Gas flow rate in 4# cell gas line	75%
Integration time, *m/z* (Q1→Q2)	90→ 90, 6.00 s; 88→ 88, 0.3 s
Sample time	53 s
APEX-Q settings	
Sample uptake rate	0.2 mL/min
Spray chamber temperature	140°C
Condenser temperature	2°C
Sweep gas (Ar)	3 L/min
Additional gas (Ar)	0.1 L/min
N_2 gas	8–10 mL/min

Table S4 The signal intensities at m/z 90-90 (Q1-Q2) for 1 ng/mL Zr during ICP-MS/MS analysis without addition of collision/reaction gas.

Introduction system	Lens type	Signal intensity ($\times 10^4$ cps)
C	X	9.6
A	X	22.3
A	S	88.0

A: APEX-Q/ACM desolvation sample introduction system. C: conventional (quartz Scott double pass spray chamber) sample introduction system

Table S5 The abundance sensitivity and method detection limit (MDL) calculated from signal intensities at m/z 88-88 and 90-90 with 10 μg/mL Sr. The gas was introduced via the 4# cell gas line.

Introduction system	Lens	Gas	Flow rate (%)	88-88 (cps)	90-90 (cps)	Abundance	MDL (pg/mL)
C	X	O_2	70	1.60×10^{9}	0.185	1.16×10^{-10}	6.77×10^{-4}
C	S	O_2	90	2.65×10^{9}	1.11	4.19×10^{-10}	2.65×10^{-4}
A	S	O_2	100	1.07×10^{10}	0.808	7.52×10^{-11}	8.43×10^{-5}
C	X	CO_2	65	1.34×10^{9}	1.67	1.24×10^{-9}	8.78×10^{-4}
C	S	CO_2	75	2.12×10^{9}	1.33	6.27×10^{-10}	9.78×10^{-4}
A	S	CO_2	95	5.49×10^{9}	4.29	7.83×10^{-10}	4.56×10^{-4}

A: APEX-Q/ACM desolvation sample introduction system. C: conventional (quartz Scott double pass spray chamber) sample introduction system

Table S6 The value comparison of measured and spiked ^{90}Sr in urine after ICP-MS/MS analysis.

^{90}Sr spiked (pg)	**^{90}Sr measured (pg)**
10 mL	
0.0218±0.0003	0.0225±0.0026
0.218±0.003	0.202±0.015
21.8±0.3	21.4±1.7
400 mL	
0.0218±0.0003	0.0213±0.0023
0.218±0.003	0.222±0.019
21.8±0.3	21.9±0.9

Expanded uncertainty (k=2), n=3, Decay corrected to the measured day.

Table S7 Concentrations (Bq/L) of ^{90}Sr in urine samples measured by the beta counting (n=3) and ICP-MS/MS methods (n=2) in the 2020 and 2023 PROCORAD program (Reference date: March 15 of the participation year).

Sample	Beta counting	ICP-MS/MS	Assigned value
20 SRA	2.56±0.21	2.68±0.45	2.72±0.13
20 SRB	-	-	-
20 SRC	5.40±0.18	5.56±0.38	5.64±0.27
23 SRA	-	-	-
23 SRB	2.81±0.03	3.30±0.51	2.79±0.16
23 SRC	5.43±0.23	5.42±0.31	4.94±0.23

-: < method detection limit.

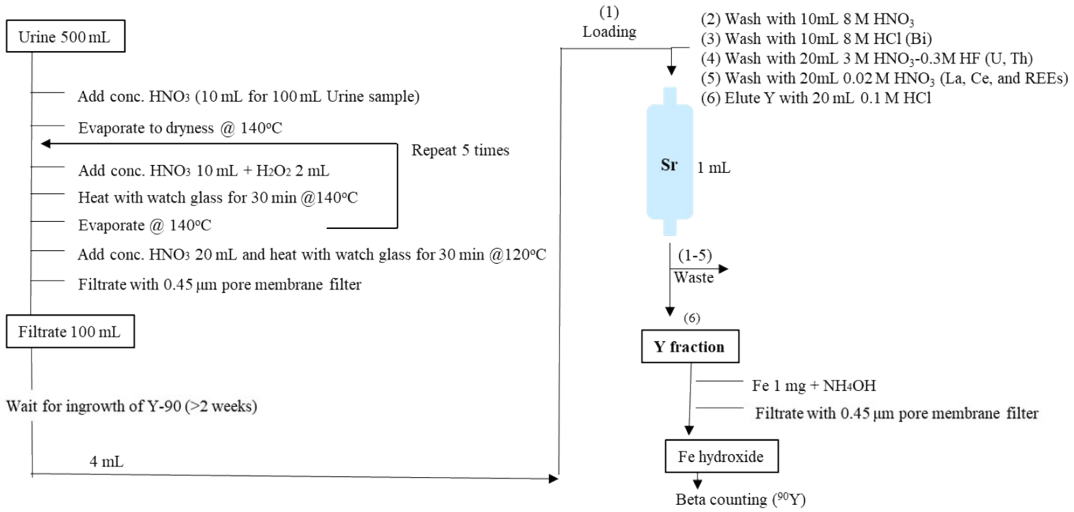

Fig. S1 Schematic diagram of determination of ^{90}Sr in urine sample by beta counting.

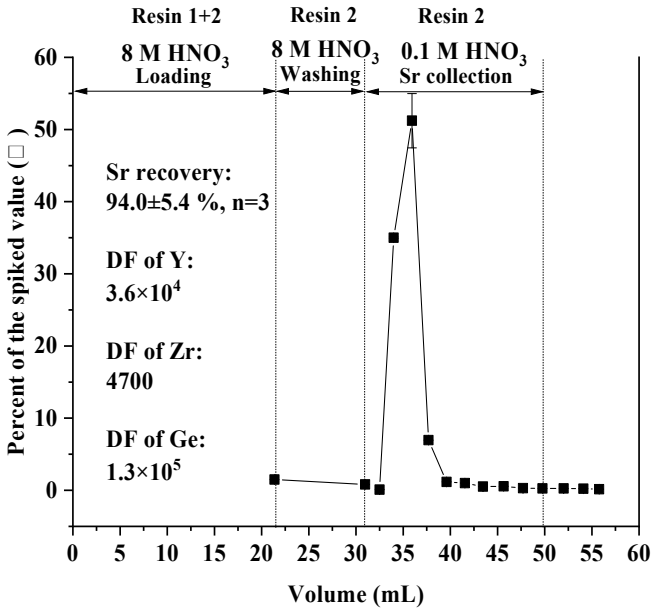

Fig. S2 The elution profiles of Sr on 2 mL DGA resin column (resin 1) and 2 mL Sr resin (resin 2). DF: decontamination factor = the amount prior to purification / the amount after purification.

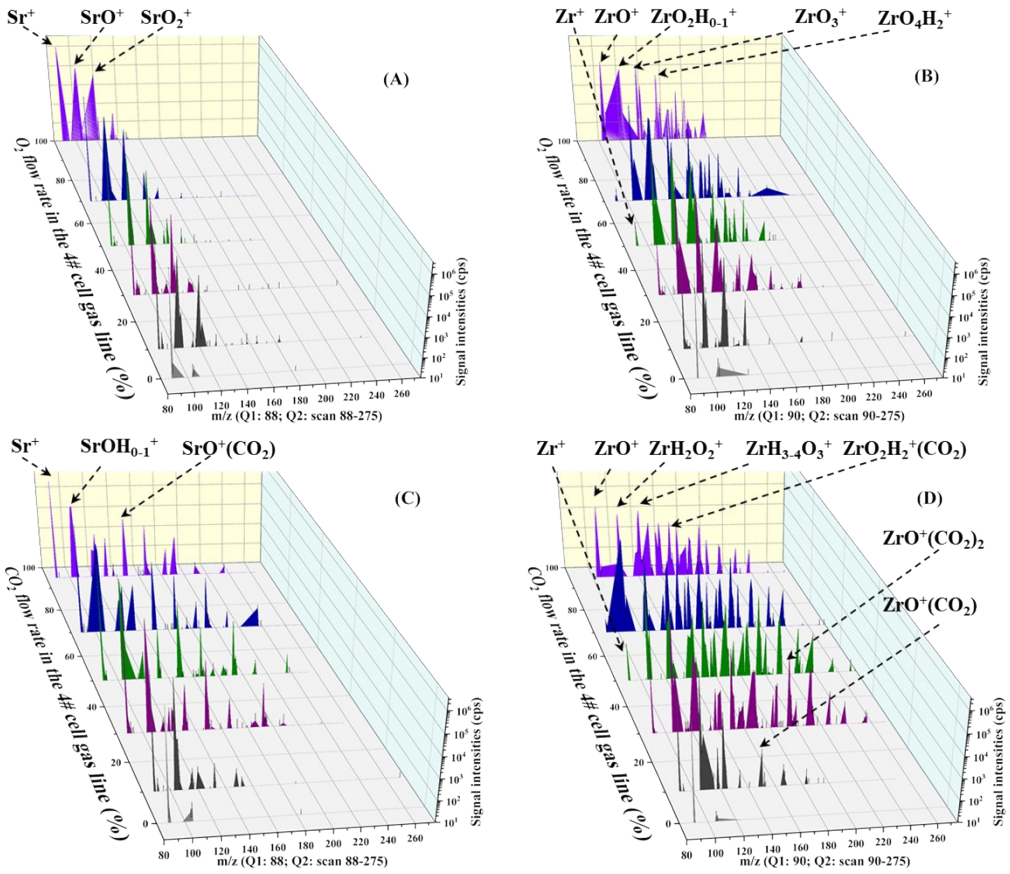

Fig. S3 Mass spectra illustrating produced ions with reaction between A) Sr and O_2; B) Zr and O_2; C) Sr and CO_2; D) Zr and CO_2. The collision/reaction gases were introduced via the $4^{\#}$ cell gas line.

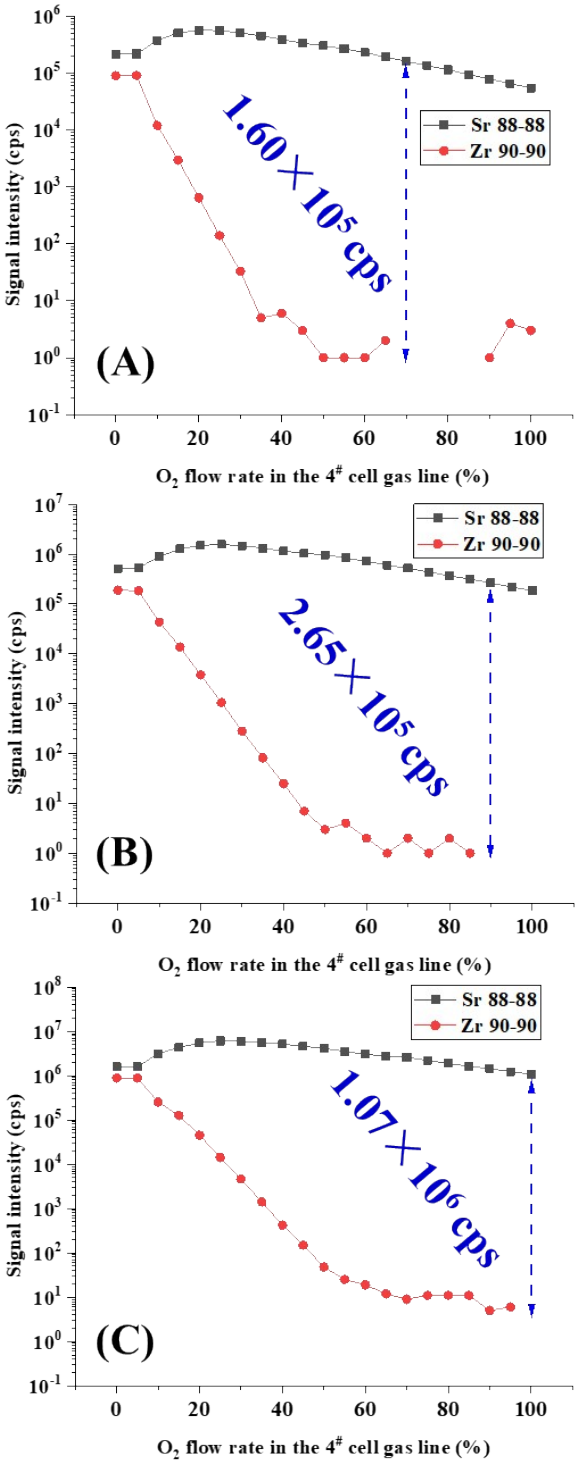

Fig. S4 The responses of 1 ng/mL Sr and Zr with the increasement of O_2 flow rate in the 4# cell gas line in on-mass mode, with the application of conventional sample introduction system＋x lens (A), conventional sample introduction system＋s lens (B), APEX-Q/ACM sample introduction system＋s lens (C). The blue data indicated the gap between signal intensities of Sr and Zr.

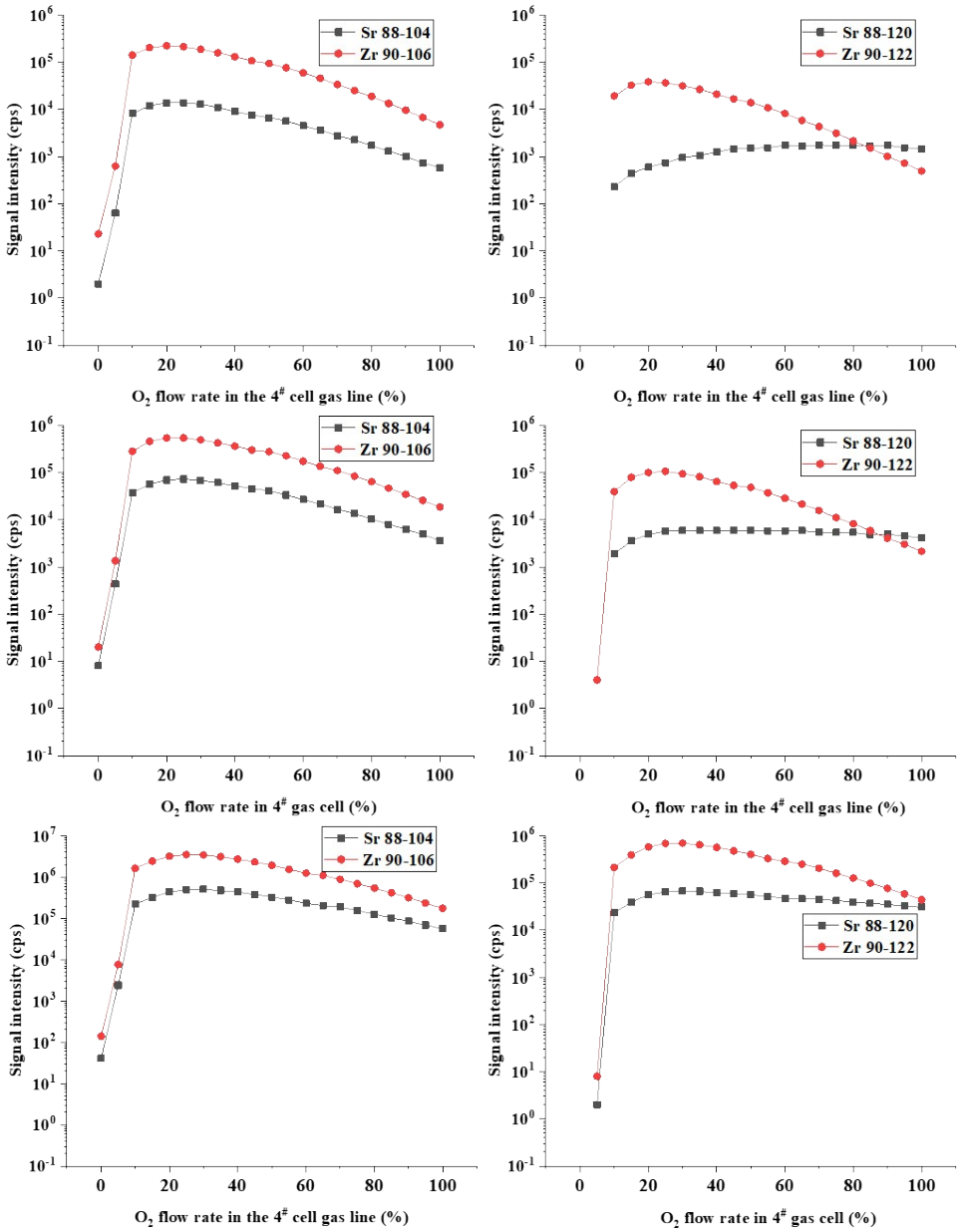

Fig. S5 The responses of 1 ng/mL Sr and Zr with the increasement of O_2 flow rate in the 4# cell gas line in mass shift modes ($M^+ \rightarrow MO^+$: left side, $M^+ \rightarrow MO_2^+$: right side), with the application of conventional sample introduction system＋x lens (upper), conventional sample introduction system＋s lens (middle), APEX-Q/ACM sample introduction system＋s type lens (bottom).

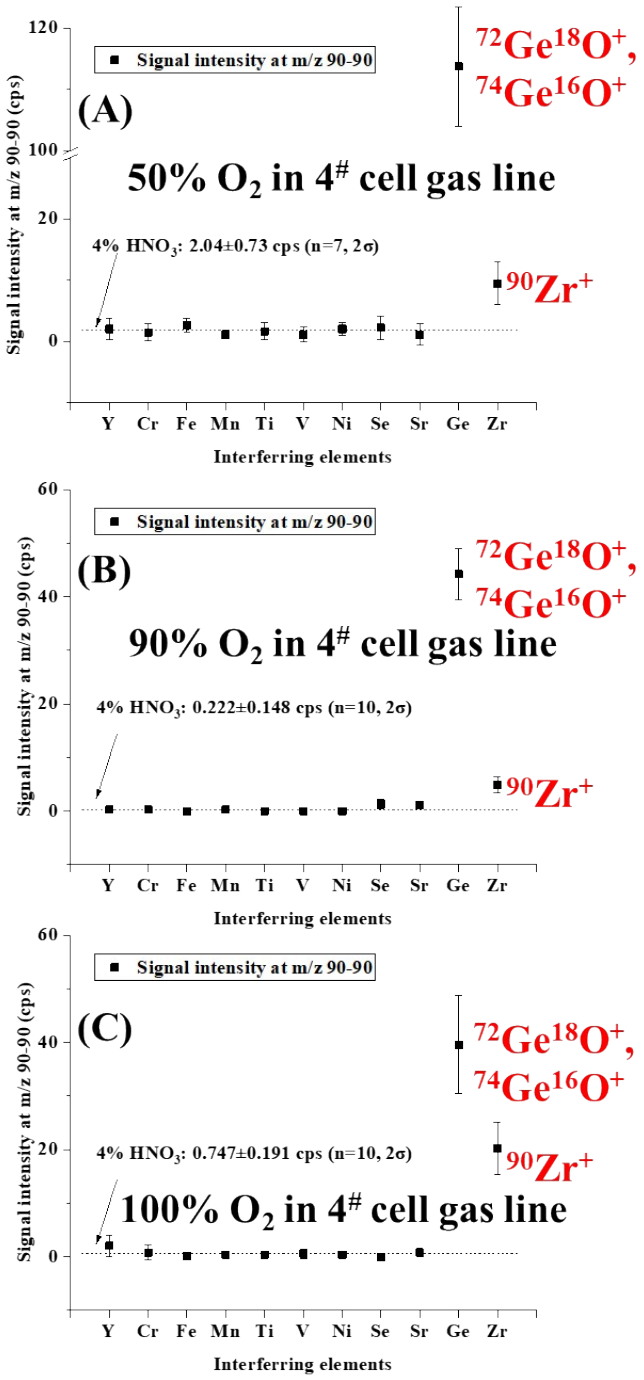

Fig. S6 The signal intensities at m/z 90-90 (Q1-Q2) using 10 μg/mL Sr and 10 ng/mL other interfering elements with the optimal O_2 flow rate in the 4# cell gas line in on-mass mode ($M^+ \rightarrow M^+$), with the application of conventional sample introduction system＋x type lens (A), conventional sample introduction system＋s type lens (B), APEX-Q/ACM sample introduction system＋s type lens (C).

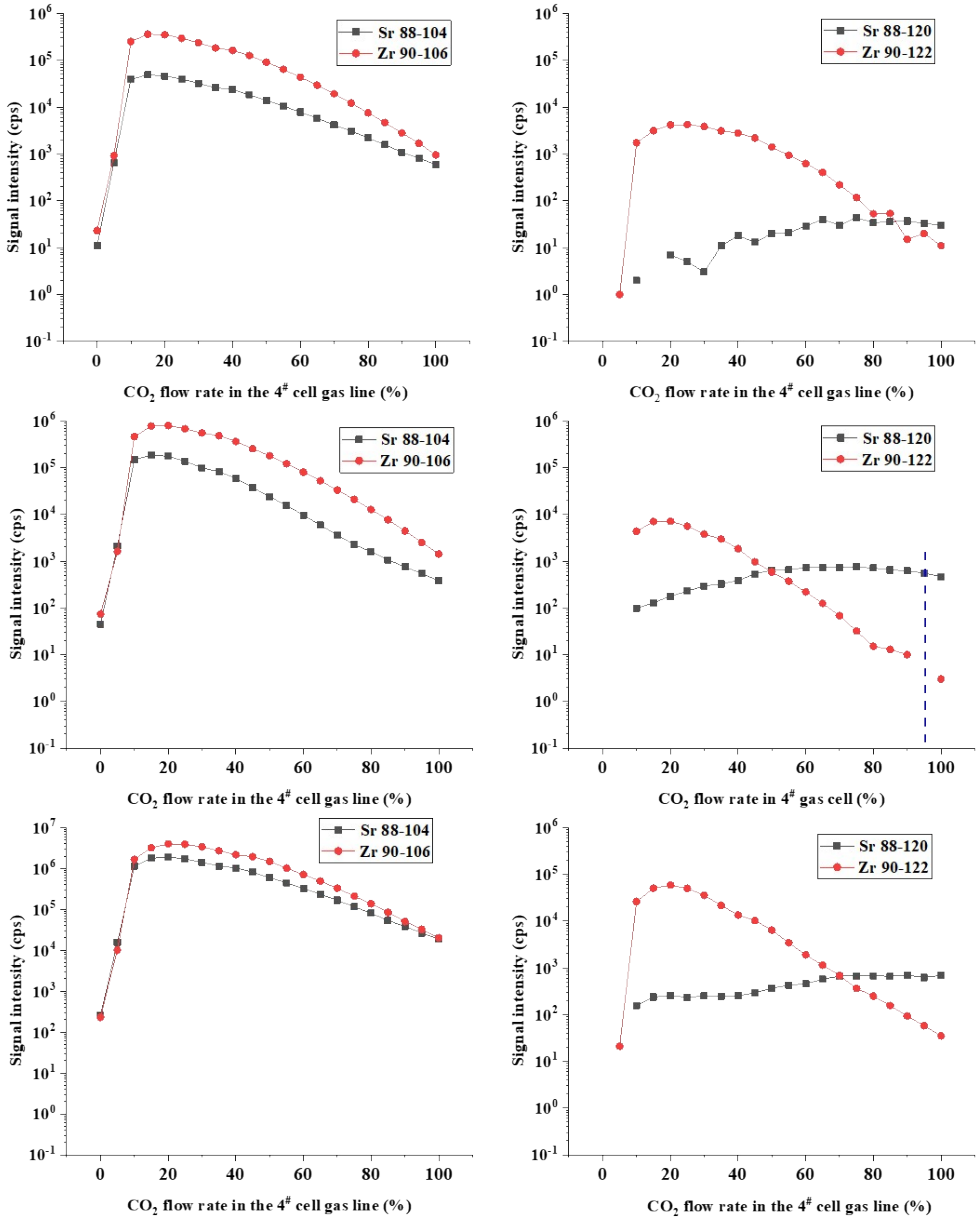

Fig. S7 The responses of 1 ng/mL Sr and Zr with the increasement of CO_2 flow rate in the 4# cell gas line in mass-shift modes ($M^+ \rightarrow MO^+$: left side, $M^+ \rightarrow MO_2^+$: right side), with the application of conventional sample introduction system＋x lens (upper), conventional sample introduction system＋s lens (middle), APEX-Q/ACM sample introduction system＋s lens (bottom).

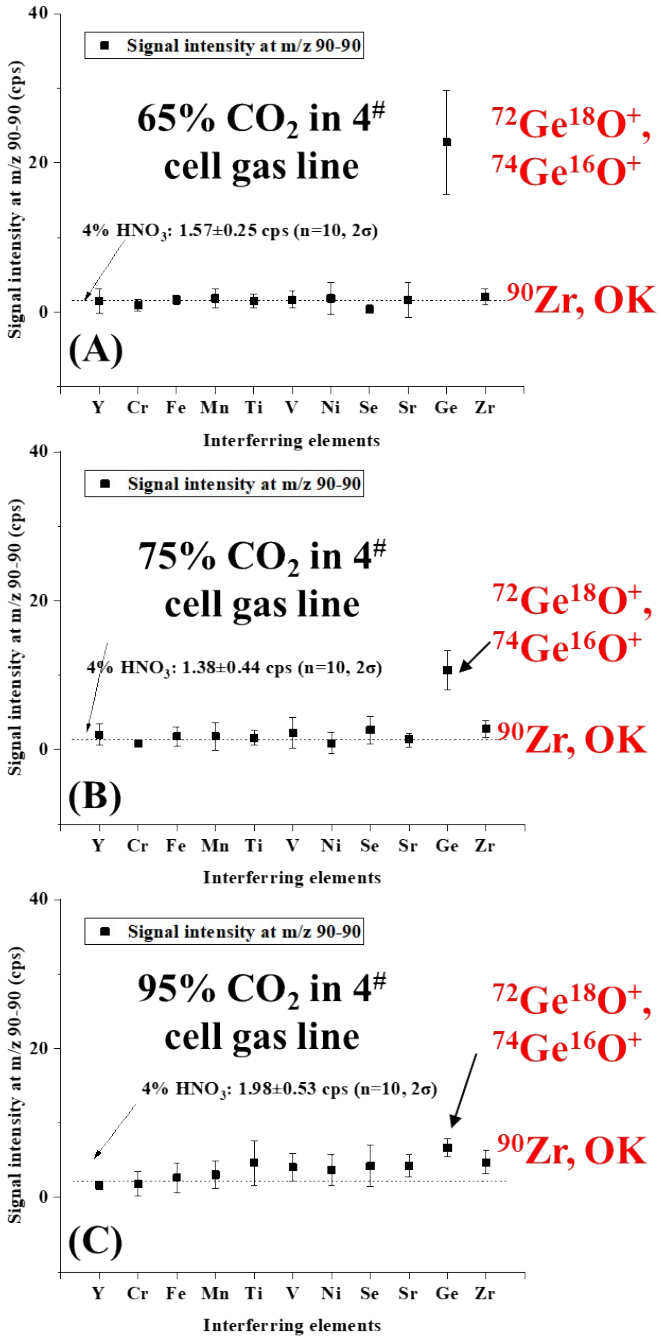

Fig. S8 The signal intensities at m/z 90-90 (Q1-Q2) using 10 μg/mL Sr and 10 ng/mL other interfering elements with the optimal CO_2 flow rate in the 4# cell gas line in on-mass mode ($M^+ \rightarrow M^+$), with the application of conventional sample introduction system＋x lens (A), conventional sample introduction system＋s lens (B), APEX-Q/ACM sample introduction system＋s lens (C). OK indicated that the signal intensity of Zr was mitigated effectively within the background signal intensity of the 4 % HNO_3 solution.

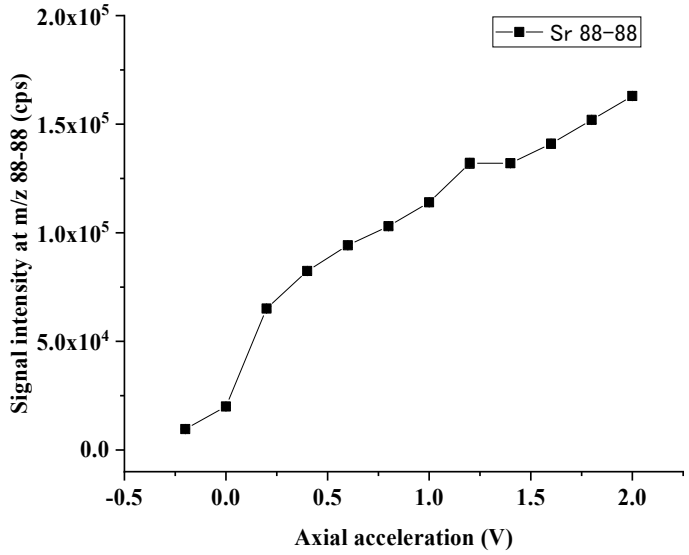

Fig. S9 The variation of signal intensities at m/z 88-88 (Q1-Q2) with variation of the axial acceleration in the collision/reaction cell, using 1 ng/mL Sr with 30% CO_2 flow rate in the 4# cell gas line in on-mass mode ($M^+ \rightarrow M^+$), with the application of conventional sample introduction system＋s lens.

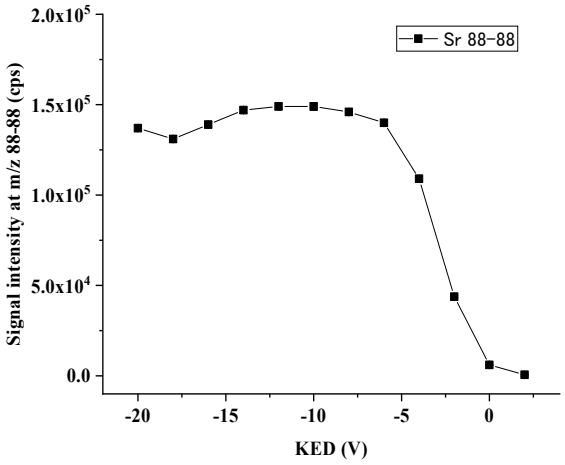

Fig. S10 The variation of signal intensities at m/z 88-88 (Q1-Q2) with variation of the kinetic energy discrimination (KED) in the collision/reaction cell, using 1 ng/mL Sr with 30% CO_2 flow rate in the 4# cell gas line in on-mass mode ($M^+ \rightarrow M^+$), with the application of conventional sample introduction system＋s lens.

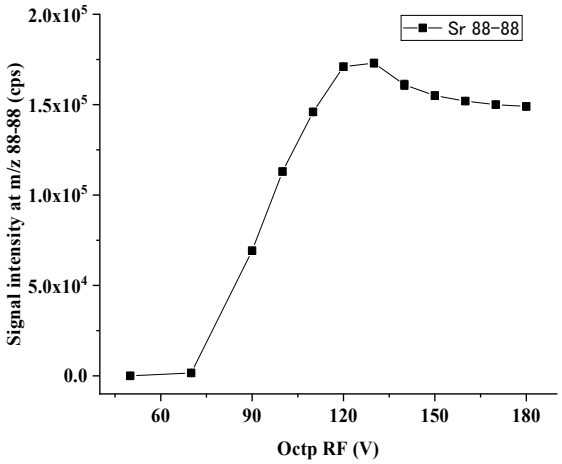

Fig. S11 The variation of signal intensities at m/z 88-88 (Q1-Q2) with variation of the Octp RF in the collision/reaction cell, using 1 ng/mL Sr with 30% CO_2 flow rate in the $4^{\#}$ cell gas line in on-mass mode ($M^+ \rightarrow M^+$), with the application of conventional sample introduction system＋s lens.

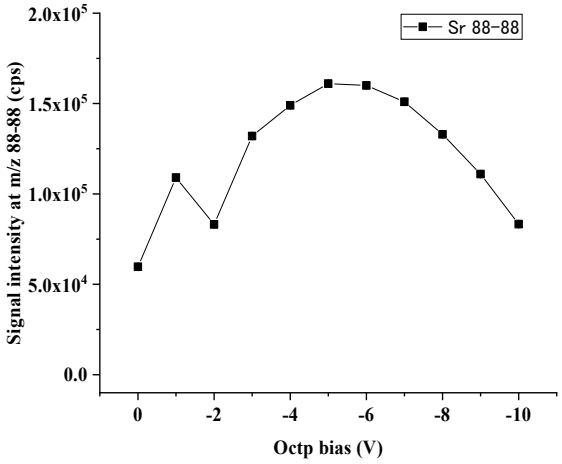

Fig. S12 The variation of signal intensities at m/z 88-88 (Q1-Q2) with variation of the Octp bias in the collision/reaction cell, using 1 ng/mL Sr with 30% CO_2 flow rate in the $4^{\#}$ cell gas line in on-mass mode ($M^+ \rightarrow M^+$), with the application of conventional sample introduction system＋s lens.

References

1. J. Morton, E. Tan, E. Leese and J. Cocker, Determination of 61 elements in urine samples collected from a non-occupationally exposed UK adult population, *Toxicol. Lett*. 2014, **231**, 179–193.
2. J. Nakagawa, Y. Tsuchiya, Y. Yashima, M. Tezuka and Y. Fujimoto, Determination of trace levels of elements in urine by inductively coupled plasma mass spectrometry, *J. Health Sci*. 2004, **50**, 164–168.
3. K. Usuda, K. Kono, T. Dote, M. Watanabe, H. Shimizu, Y. Tanimoto and E. Yamadori, An overview of boron, lithium, and strontium in human health and profiles of these elements in urine of Japanese, *Environ. Health Prev. Med*. 2007, **12**, 231–237.